Effective g factor of 2D holes in strained Ge quantum wells

I. L. Drichko, A. A. Dmitriev, V. A. Malysh, I. Yu. Smirnov, H. von Känel, M. Kummer, D. Chrastina, and G. Isella

Citation: Journal of Applied Physics **123**, 165703 (2018); doi: 10.1063/1.5025413

View online: https://doi.org/10.1063/1.5025413

View Table of Contents: http://aip.scitation.org/toc/jap/123/16

Published by the American Institute of Physics

Effective g factor of 2D holes in strained Ge quantum wells

I. L. Drichko,[1] A. A. Dmitriev,[1,2] V. A. Malysh,[1] I. Yu. Smirnov,[1,a)] H. von Känel,[3] M. Kummer,[3] D. Chrastina,[4] and G. Isella[4]
[1]*Ioffe Institute, 26 Politekhnicheskaya, 194021 St. Petersburg, Russia*
[2]*Department of Nanophotonics and Metamaterials, ITMO University, 49 Kronverksky Pr., 197101 St. Petersburg, Russia*
[3]*Laboratory for Solid State Physics, ETH Zurich, Otto-Stern-Weg 1, CH-8093 Zurich, Switzerland*
[4]*INFM and L-NESS Dipartimento di Fisica, Politecnico di Milano, Polo Regionale di Como, Via Anzani 52, I-22100 Como, Italy*

(Received 9 February 2018; accepted 6 April 2018; published online 24 April 2018)

The effective g-factor of 2D holes in modulation doped p-SiGe/Ge/SiGe structures was studied. The AC conductivity of samples with hole densities from 3.9×10^{11} to $6.2 \times 10^{11}\,\mathrm{cm}^{-2}$ was measured in perpendicular magnetic fields up to 8 T using a contactless acoustic method. From the analysis of the temperature dependence of conductivity oscillations, the $g_\perp$-factor of each sample was determined. The $g_\perp$-factor was found to be decreasing approximately linearly with hole density. This effect is attributed to the non-parabolicity of the valence band. *Published by AIP Publishing*. https://doi.org/10.1063/1.5025413

I. INTRODUCTION

Over the last few years, modulation doped SiGe/Ge/SiGe structures with a 2D hole gas have constantly been a subject of interest, due to their high hole mobilities and epitaxial compatibility with Si. Recently, homogenous samples with hole mobility high enough to observe the integer and even the fractional quantum Hall effect have become available.[1,2]

In such structures, the lattice constant mismatch between SiGe and Ge leads to compressive strain in the Ge quantum well. This strain lifts the degeneracy of the heavy hole and light hole subbands in the Γ-point. In the relevant case of compressive strain, the heavy hole subband lies higher in energy, which gives the opportunity to investigate the properties of only heavy holes. The subbands interact with each other, however, and this interaction gives rise to valence band non-parabolicity. It can manifest itself through hole density dependencies of effective mass and g-factor. The former has been studied extensively.[3,4]

Because of the large g-factor of bulk Ge ($g = 20.4$), the $g_\perp$-factor of 2D holes in Ge quantum wells is also expected to be large and to depend on the hole density due to valence band non-parabolicity. However, until very recently, only a few values of the $g_\perp$-factor in SiGe/Ge/SiGe structures have been present in literature.[1,5–7] The first investigation of the $g_\perp$-factor dependence on hole density was published in 2017.[8] Its authors studied the $g_\perp$-factor of 2D holes in a heterostructure field-effect transistor with low hole densities from 1.4×10^{10} to $1.3 \times 10^{11}\,\mathrm{cm}^{-2}$. The aim of the present work is to continue the investigation of the $g_\perp$-factor in the region of higher hole densities.

a)ivan.smirnov@mail.ioffe.ru

II. EXPERIMENTAL RESULTS AND DISCUSSION

A. Samples

We have studied modulation-doped single p-Si_xGe_{1-x}/Ge/Si_xGe_{1-x} quantum wells with hole densities from 3.9×10^{11} to $6.2 \times 10^{11}\,\mathrm{cm}^{-2}$. They had all been grown on Si(001) substrates using low-energy plasma-enhanced chemical vapor deposition (LEPECVD).[9] Symmetrically and asymmetrically doped samples have both been studied. A summary of the samples is presented in Table I.

B. Method

We used the contactless acoustic method[10,11] to determine the complex AC conductance of the 2D hole gas, $\sigma = \sigma_1 - i\sigma_2$. In the present work, however, we were generally focused on the real part, σ_1, of the complex conductance.

A schematic of the experiment setup is shown in Fig. 1. The samples are mounted onto a $LiNbO_3$ piezoelectric crystal with a pair of interdigital transducers (IDTs), which induce a surface acoustic wave (SAW) on the crystal surface. A SAW-induced AC electric field penetrates the sample and interacts with charge carriers (holes). As a result, the SAW

TABLE I. Summary of the samples.

Sample	Hole density (cm^{-2})	QW width (nm)	x	Doping layers
7989-2	3.9×10^{11}	13	0.3	At each side
6745-3	4.5×10^{11}	15	0.3	Single-sided
8005	4.5×10^{11}	13	0.3	At each side
6745-2	4.9×10^{11}	15	0.3	Single-sided
6777-2	5.2×10^{11}	15	0.3	Single-sided
K6016	6.0×10^{11}	20	0.4	Single-sided
7974-2	6.2×10^{11}	13	0.3	At each side

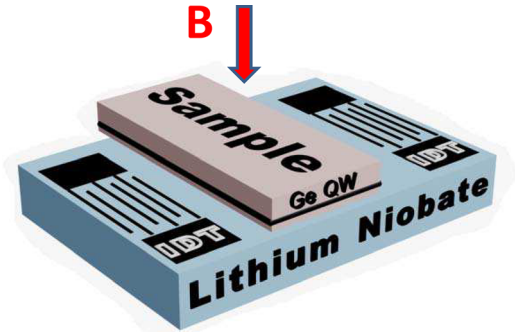

FIG. 1. A schematic of the experimental setup.

attenuation Γ and velocity v both acquire additional contributions, which can be related to the complex conductance σ with the following formulas:[12]

$$\Gamma = 8.68q\frac{K^2}{2}A\frac{\Sigma_1}{\Sigma_1^2+[\Sigma_2+1]^2},\frac{\mathrm{dB}}{\mathrm{cm}},$$
$$\frac{\Delta v}{v_0} = \frac{K^2}{2}A\frac{[\Sigma_2+1]}{\Sigma_1^2+[\Sigma_2+1]^2},$$
$$\Sigma_i = \frac{4\pi t(q)}{\varepsilon_S v_0}\sigma_i, i=1,2,$$
$$A = 8b(q)[\varepsilon_1+\varepsilon_0]\varepsilon_0^2\varepsilon_S\exp\left(-2q(a+d)\right), \quad (1)$$

where K^2 is the electromechanical coupling constant for $LiNbO_3$; q and v_0 are the SAW wave vector and velocity in $LiNbO_3$, respectively; a is the vacuum gap between the $LiNbO_3$ crystal and the sample; d is the distance between the sample surface and the QW layer; ε_1, ε_0, and ε_s are the dielectric constants of $LiNbO_3$, of vacuum, and of the semiconductor, respectively; and b and t—are complex functions of q, a, d, ε_0, ε_1, and ε_s.

Measurements of the SAW attenuation Γ and velocity v have been performed in magnetic fields up to 8 T perpendicular to the QW plane and at temperatures from 1.7 to 4.2 K. Figure 2 shows Γ and v plotted as functions of magnetic field. Both curves demonstrate oscillations. The real part σ_1 of the complex conductance was then obtained from these measurements by solving Eq. (1). Figure 3 shows the conductance σ_1 of sample 6777–2 calculated in this way, as a function of magnetic field at different temperatures. The

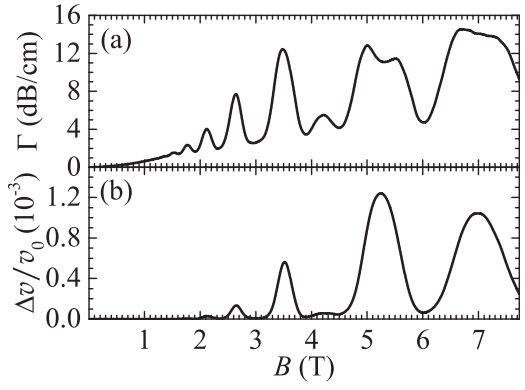

FIG. 2. Dependence of the surface acoustic wave attenuation (a) and velocity (b) for the sample 6777-2 on the magnetic field; $f = 30$ MHz, $T = 1.8$ K.

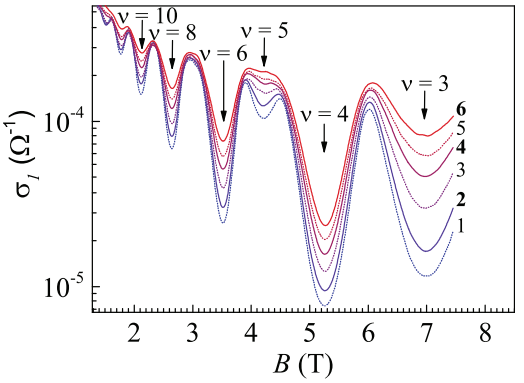

FIG. 3. Dependence of the real part of AC conductance of sample 6777-2 on the magnetic field at different temperatures: 1–1.8 K, 2–2.1 K, 3–2.7 K, 4–3.2 K, 5–3.7 K, and 6–4.2 K; $f = 30$ MHz. ν is the filling factor.

curves demonstrate Shubnikov–de Haas oscillations, which evolve into the characteristic oscillations of the integer quantum Hall effect regime in stronger fields. The same picture has been observed with all samples.

C. Determination of g-factor

The analysis of the temperature dependence of the conductance at the minima of the oscillations allows us to determine the $g_\perp$-factor using the following procedure. We have found that at each oscillation minimum, there is a temperature range where the conductance is characterized by a constant activation energy Δ,

$$\sigma_1 \sim \exp\left(-\frac{\Delta}{2kT}\right). \quad (2)$$

We have then determined Δ for each minimum by performing linear fitting of the dependence of $\ln\sigma_1$ on T^{-1}.

On the other hand, one can write down expressions for activation energy considering the Landau level structure at the minima of oscillations, where the Fermi level is halfway between adjacent Landau levels. Even and odd filling factors correspond to orbital and spin splitting of Landau levels, respectively, as is shown in Fig. 4. Taking the Landau level

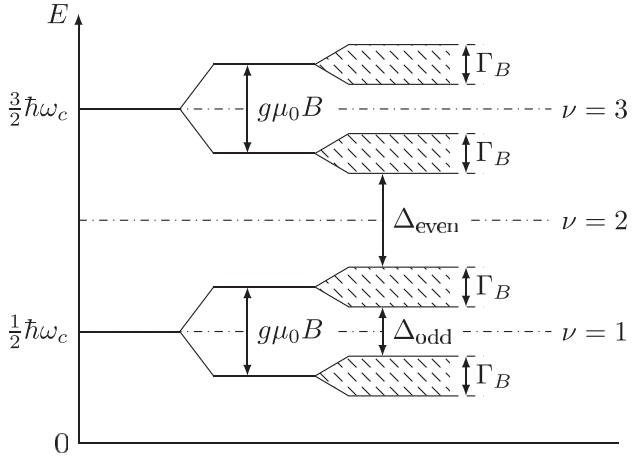

FIG. 4. Landau level structure at an oscillation minimum. ν is the filling factor. The hatched areas denote the Landau level broadening Γ_B.

broadening Γ_B into account as $\Gamma_B = C\sqrt{B}$ (Ref. 13), one can express activation energies for even and odd filling factors as

$$\Delta_{\text{odd}} = g_\perp \mu_0 B - \Gamma_B, \tag{3}$$

$$\Delta_{\text{even}} = \hbar\omega_c - g_\perp \mu_0 B - \Gamma_B, \tag{4}$$

where $\hbar\omega_c$ is the cyclotron energy and μ_0 is the Bohr magneton. Equations (3) and (4) are then solved for $g_\perp$ and C for each $(\Delta_{\text{even}}, \Delta_{\text{odd}})$ pair.

Table II shows the values obtained for sample 6777–2. On can see from the table that the $g_\perp$-factor does not depend on the magnetic field within our experimental error (estimated as 10%–15%).

Using the procedure described above, we have obtained the values of $g_\perp$-factor for every sample; the results are listed in Table III. It is worth mentioning that the effective mass dependence on the hole density has been neglected in our calculations, and a constant value of $m^* = 0.1m_0$, where m_0 is the free electron mass, has been taken instead. This approximation is valid because the effective mass changes only by 15% within the range of carrier densities studied in the present work.[4]

D. Discussion

Figure 5 summarizes the results of several studies of the $g_\perp$-factor value in SiGe/Ge/SiGe structures, including those of the present work. We attribute the decrease in the $g_\perp$-factor to valence band non-parabolicity, which is due to the mixing of HH and LH states away from the zone center. At the center of the valence band, the $g_\perp$-factor of 2D holes should be approximately equal to the g-factor of heavy holes in bulk Ge ($g = 20.4$). With growing hole density, the $g_\perp$-factor is expected to decrease from the band-center value.

The reason is that in the presence of the non-zero momentum component $p_\parallel$ along the QW plane, the hole state is no longer the pure heavy hole state $|\pm\frac{3}{2}\rangle$ but contains an admixture of the light hole state $|\pm\frac{1}{2}\rangle$. The degree of this admixture is roughly proportional to $p_\parallel^2$, which, at the Fermi level, is proportional to the hole density. Thus, the $g_\perp$-factor becomes a combination of the $g_\perp$-factors of heavy and light holes, taken with weights which are proportional to fractions of heavy and light holes in the observed state.[14] The result of a calculation[14] based on the 4×4 $\mathbf{k}\cdot\mathbf{p}$ Hamiltonian in the infinite well approximation is shown with the blue dashed line in Fig. 5. As is seen from the figure, this theoretical curve fails to describe the experimental results.

TABLE II. Values of the effective $g_\perp$-factor and the Landau level broadening factor C, calculated for different pairs of conductance oscillation minima (sample 6777-2).

ν_{odd}	ν_{even}	$g_\perp$	C (meV/T$^{1/2}$)
3	6	8.5	0.8
3	8	8.5	0.8
3	10	8.3	0.8
3	12	8.4	0.8
5	6	8.4	0.8
5	8	8.4	0.8
5	10	8.2	0.8
5	12	8.2	0.8

TABLE III. Values of the effective $g_\perp$-factor obtained for different samples.

Sample	Hole density (cm^{-2})	$g_\perp$-factor
7989-2	3.9×10^{11}	10 ± 2
6745-3	4.5×10^{11}	9.0 ± 1.4
8005	4.5×10^{11}	8.9 ± 1.5
6745-2	4.9×10^{11}	8.9 ± 1.4
6777-2	5.2×10^{11}	8.4 ± 1.3
K6016	6.0×10^{11}	6.9 ± 1.1
7974-2	6.2×10^{11}	7.3 ± 1.2

Several numerical calculations that were based on a more rigorous model with the 6×6 $\mathbf{k}\cdot\mathbf{p}$ Hamiltonian have been made to explain the density dependence of the effective mass.[4,15] In these studies, along with the split-off (SO) band, self-consistent potential profiles and the effects of strain due to the lattice mismatch between Ge and SiGe were also taken into account. The results of these computations show good agreement with the experimental dependence of the effective mass on density. The structures studied in Ref. 4 have almost the same parameters as those investigated in the present work, so we used the results of calculations from Ref. 4 to interpret the $g_\perp$-factor dependence on density as follows.

As the density dependencies of both effective mass and $g_\perp$-factor of heavy holes have the same microscopic nature, they can be related to each other as follows:[16]

$$|g_\perp| = \left|2\left(-3\mathcal{K} + (\gamma_1 + \gamma_2) - \frac{m_0}{m^*}\right)\right|, \tag{5}$$

where m_0 is the free electron mass, $\gamma_1 = 13.38$, $\gamma_2 = 4.26$, and $\mathcal{K} = 3.41$ are the Luttinger parameters of Ge.[17] The dependence of the $g_\perp$-factor on density was evaluated from the theoretical dependence of the effective mass on density[4] by means of formula (5). The result is shown with the solid line in Fig. 5. As is seen, it describes the experimental data with good agreement. Thus, the observed experimental $g_\perp$-factor

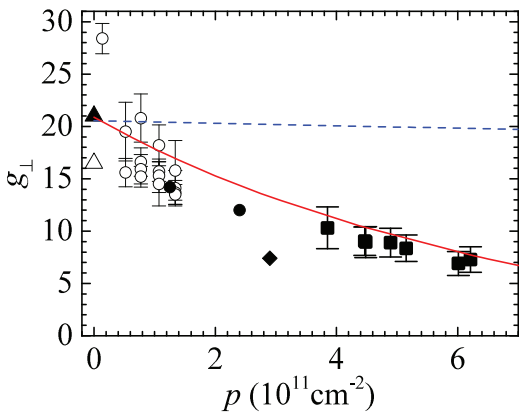

FIG. 5. Density dependence of the $g_\perp$-factor: (▲)—g-factor of bulk Ge; (◆)—Ref. 1, the Landau level broadening is neglected; (●)—Refs. 5 and 6; (△)—Ref. 7; (◯)—Ref. 8; and (■)—the present work. The dashed line shows the result of theoretical calculations based on the 4×4 $\mathbf{k}\cdot\mathbf{p}$ model.[14] The solid line shows the $g_\perp$-factor evaluated with formula (5) from the theoretical computation of the effective mass in the 6×6 $\mathbf{k}\cdot\mathbf{p}$ model.[4]

dependence on density can be attributed to the interaction between HH, LH, and SO subbands, as affected by the strain present in the quantum well.

III. CONCLUSIONS

We have performed contactless conductance measurements on the 2D hole gas in p-SiGe/Ge/SiGe structures by means of acoustic spectroscopy, and determined the effective $g_{\perp}$-factor. It was found that the $g_{\perp}$-factor depends approximately linearly on the hole density, but is independent of the magnetic field, the Si content x in the spacer layers, and the character of the modulation doping (see Table I). The observed change is attributed to valence band nonparabolicity.

ACKNOWLEDGMENTS

We are grateful to A. V. Nenashev, S. A. Tarasenko, M. V. Durnev, and N. G. Shelushinina for useful discussions of the experimental results. Author A.A.D. also acknowledges the support from the Government of the Russian Federation (Grant No. 074-U01).

[1]Q. Shi, M. A. Zudov, C. Morrison, and M. Myronov, "Spinless composite fermions in an ultrahigh-quality strained Ge quantum well," Phys. Rev. B **91**, 241303 (2015).
[2]O. A. Mironov, N. d'Ambrumenil, A. Dobbie, D. R. Leadley, A. V. Suslov, and E. Green, "Fractional quantum hall states in a Ge quantum well," Phys. Rev. Lett. **116**, 176802 (2016).
[3]T. Irisawa, M. Myronov, O. A. Mironov, E. H. C. Parker, K. Nakagawa, M. Murata, S. Koh, and Y. Shiraki, "Hole density dependence of effective mass, mobility and transport time in strained Ge channel modulation-doped heterostructures," Appl. Phys. Lett. **82**, 1425–1427 (2003).
[4]B. Rössner, H. von Känel, D. Chrastina, G. Isella, and B. Batlogg, "Effective mass measurement: The influence of hole band nonparabolicity in SiGe/Ge quantum wells," Semicond. Sci. Technol. **22**, S191 (2007).
[5]Y. G. Arapov, G. I. Harus, N. G. Shelushinina, M. V. Yakunin, V. N. Neverov, O. A. Kuznetsov, L. Ponomarenko, and A. De Visser, "Nonmonotonic temperature dependence of the resistivity of p-Ge/Ge1-xSix in the region of the metal–insulator transition," Sov. J. Low Temp. Phys. **30**, 867–870 (2004).
[6]Y. G. Arapov, S. V. Gudina, I. V. Karskanov, V. N. Neverov, G. I. Harus, and N. G. Shelushinina, "Contributions of the electron–electron interaction and weak localization to the conductance of p-Ge/Ge1-xSix heterostructures," Sov. J. Low Temp. Phys. **33**, 160–164 (2007).
[7]A. V. Nenashev, A. V. Dvurechenskii, and A. F. Zinovieva, "Wave functions and g factor of holes in Ge/Si quantum dots," Phys. Rev. B **67**, 205301 (2003).
[8]T. M. Lu, C. T. Harris, S.-H. Huang, Y. Chuang, J.-Y. Li, and C. W. Liu, "Effective g factor of low-density two-dimensional holes in a Ge quantum well," Appl. Phys. Lett. **111**, 102108 (2017).
[9]G. Isella, D. Chrastina, B. Rössner, T. Hackbarth, H.-J. Herzog, U. König, and H. von Känel, "Low-energy plasma-enhanced chemical vapor deposition for strained Si and Ge heterostructures and devices," Solid-State Electron. **48**, 1317–1323 (2004).
[10]A. Wixforth, J. P. Kotthaus, and G. Weimann, "Quantum oscillations in the surface-acoustic-wave attenuation caused by a two-dimensional electron system," Phys. Rev. Lett. **56**, 2104–2106 (1986).
[11]I. L. Drichko, A. M. Diakonov, E. V. Lebedeva, I. Y. Smirnov, O. A. Mironov, M. Kummer, and H. von Känel, "Acoustoelectric effects in very high-mobility p-SiGe/Ge/SiGe heterostructure," J. Appl. Phys. **106**, 094305 (2009).
[12]V. D. Kagan, "Propagation of a surface acoustic wave in a layered system containing a two-dimensional conducting layer," Sov. Phys. Semicond. **31**, 407–410 (1997).
[13]P. T. Coleridge, "Magnetic field induced metal–insulator transitions in p-SiGe," Solid State Commun. **127**, 777–782 (2003).
[14]A. V. Nenashev, private communication (25 November 2017).
[15]R. Winkler, M. Merkler, T. Darnhofer, and U. Rössler, "Theory for the cyclotron resonance of holes in strained asymmetric Ge-SiGe quantum wells," Phys. Rev. B **53**, 10858–10865 (1996).
[16]T. Wimbauer, K. Oettinger, A. L. Efros, B. K. Meyer, and H. Brugger, "Zeeman splitting of the excitonic recombination in $In_xGa_{1-x}As$/GaAs single quantum wells," Phys. Rev. B **50**, 8889–8892 (1994).
[17]E. L. Ivchenko and G. Pikus, *Superlattices and Other Heterostructures: Symmetry and Optical Phenomena* (Springer Science & Business Media, 2012), Vol. 110.